DENOISING OF ECG SIGNALS USING WAVELETS

A DISSERTATION

Submitted in partial fulfillment of the

Requirements for the award of the degree

Of

MASTER OF TECHNOLOGY

in

ELECTRICAL ENGINEERING

(Specialization in Instrumentation and Signal Processing)

By

JASVIN DURYODHAN RAUT

(13528004)

DEPARTMENT OF ELECTRICAL ENGINEERING

INDIAN INSTITUTE OF TECHNOLOGY ROORKEE

ROORKEE-247667 (INDIA)

JUNE-2016

CANDIDATE'S DECLARATION

I hereby certify that the work delivered in this dissertation entitled **"DENOISING OF ECG SIGNALS USING WAVELETS"** submitted in partial fulfillment of the requirement of award of Degree of **Master of Technology** in Electrical Engineering with specialization in **Instrumentation and Signal processing**, submitted to the **Department of Electrical Engineering**, **Indian Institute of Technology, Roorkee** is an authentic record of the work carried out during a period from July 2014 to June 2016 under the guidance and supervision of **Dr. AMBALIKA SHARMA**, Department of Electrical Engineering, Indian Institute of Technology, Roorkee. The matter presented in this dissertation has not been submitted by me for the award of any other degree of this institute or any other institute.

Date:

Place: Roorkee **JASVIN DURYODHAN RAUT**

(13528004)

CERTIFICATE

This is to certify that the above statement made by the candidate is correct to best of my knowledge.

Dr. AMBALIKA SHARMA
Assistant Professor
Department of Electrical Engineering,
Indian Institute of Technology Roorkee
Roorkee-247667, India

ABSTRACT

The electrocardiogram (ECG) is the graphical recording of the electrical potential of heart versus time. The analysis of ECG signal has a great importance in the detection of cardiac abnormalities. The electrocardiographic signals are complex in nature and are often contaminated by noise from diverse sources. Noises that comes in recording of the basic electrocardiogram are instrumentation noise, power line interference, external electromagnetic field interference, respirational movements and noise due to random body movements. These noises can be classified according to their frequency content. It is necessary to reduce these kind of disturbances in ECG signal to improve accuracy and reliability.

In the present work denoising of ECG signals has been carried out. Discrete Wavelet Transform (DWT) based methodology are used for noise removal. In order to evaluate the performance of the technique the algorithm has been applied to twenty normal records of the MIT-BIH database each of more than four thousand sample points. The performance of compression is evaluated in terms of Signal to Noise Ratio (SNR), Mean Square Error (MSE) and Percentage Root Mean Square Difference (PRD). In wavelet transform, a signal is analyzed and expressed as a linear combination of the summation of the product of the wavelet coefficients and mother wavelet. The wavelet decomposition offers an excellent resolution both in time and frequency domain.

ACKNOWLEDGEMENT

First of all, I would like to thank Almighty God for their blessing and for all the achievements in my life. I wish to express my deep sense of gratitude and sincere thanks to my respected guide Dr. Ambalika Sharma, Assistant Professor, Department of Electrical Engineering, Indian Institute of Technology Roorkee for giving inspiration, expert guidance, moral support and encouragement throuout this work. I could not have imagined having a better advisor and mentor for my Master's study.

My sincere thanks to the Head, Electrical Engineering Department, IIT Roorkee for providing necessery research facilities to carry out this work. I extend my thanks to all faculty members of department for their advices and valuable suggstions, and motivations provided by are duly acknowledged. I dedicate this dissertation to my family for their unremittinggly support during my years of study.

JASVIN DURYODHAN RAUT

13528004

Table of Contents

List of Figures

List of Tables

ABBREVIATION

ECG	Electrocardiography
EMG	Electromyography
DCT	Discrete Cosine Transform
DWT	Discrete Wavelet Transform
IDWT	Inverse Discrete Wavelet Transform
FFT	Fast Fourier Transform
CR	Compression Ratio
PRD	Percentage RMS Difference
SNR	Signal to Noise Ratio
MIT/BIH	Massachusetts Institute of Technology- Beth Israel Hospital

CHAPTER 1

INTRODUCTION

1.1 Introduction

Everywhere around us are signals that need to be analyzed. Seismic tremors, human speech, engine vibrations, medical images, financial data, music, and many other types of signals. One of the most important one is electrocardiogram signal. ECG is the record of the electrical potentials produced by the heart. The electrical wave is generated by depolarization and repolarization of certain cells due to movement of Na+ and k+ ions in the blood. It is a graphical demonstration of the deviation of bio-potential versus time. The leads are placed on precise locations of the body of the person to record ECG either on graph paper or on monitors. The ECG is acquired by a non-invasive technique, i.e. placing electrodes at standardized locations on the skin of the patient. The ECG signal and heart rate reflects the cardiac health of human heart. Any disorder in heart rate or rhythm or change in the morphological pattern of ECG signal is an indication of cardiac arrhythmia. It is detected and diagnosed by analysis of the recorded ECG waveform. There are five waves in ECG signal, a P wave, QRS complex and a T wave corresponding to atrial depolarization, ventricular depolarization and rapid repolarization of ventricles. The amplitude and duration of the P-QRS-T-U wave contains useful information about the nature of disease related to heart.

In clinical environment during acquisition, the ECG signal encounters various types of artifacts. The ones of primary interest are power line interference, external electromagnetic field interference, noise due to random body movements and respirational movements, electrode contact noise, electromyography (EMG) noise, and instrumentation noise. These noises degrade the signal quality, frequency resolution and strongly affect the morphology of ECG signal containing important information. It is

essential to reduce disturbances in ECG signal and improve the accuracy and reliability for better diagnosis.

Many methods have been implemented to remove the noise from noisy ECG signal. The basic method is to pass the signal through high pass, low pass and notch filters. But these filters are examples of static filters. One of the biggest disadvantages of this static filter is that these also remove some important frequency components in the vicinity of cut off frequency. The static filters have fixed filter coefficients. It is difficult to reduce the instrumentation noise with fixed filter coefficients, because the time varying behaviour of this noise is not exactly known. To overcome the limitations of static filters, different adaptive filtering methods have been developed. ECG denoising is done by wavelet based filters.

1.2 Literature Survey

During past few years, various contributions have been made in literature regarding noise removal, beat detection and classification of ECG signal. Most of them use either time or frequency domain representation of the ECG waveforms. ECG signal is an important source for diagnosis of cardiac patients.

In the paper "Denoising of ECG Signal with Different Wavelets", Inderbir Kaur, Rajni and Gaurav Sikri have shown comparison between Wavelets. Discrete Wavelet Transform is used to denoise the signal. It also shows a comparison between wavelets. According to performance parameters calculated it is shown that the Bior3.1 Wavelet is better than other due to higher PSNR, lower MSE and PRD than other wavelets[1].

In the paper "Comparative Study of ECG Signal Denoising and R-peak Registration Methods", Vikramjit Singh, Simranjeet Kaur and Aditi Gupta present the comparative study of ECG signal denoising methods and R-peak registration. They also show Denoising using discrete wavelet transform shows good result in context with adaptive thresholding[2].

In the paper “Denoising ECG Signal Using Different Wavelet Families and Comparison with Other Techniques” Uzzal Biswas, Kazi Reyadul Hasan, Biswajit Sana and Md. Maniruzzaman shown analysis of original, mixed and denoised ECG signal, both in time and frequency domains shows that wavelet transform reduces the 50 Hz power line interference more accurately. MSE and PSD values of wavelet transform is too good than that of adaptive NLMS and traditional notch filters [3].

In the paper “A Review on feature extraction and denoising of ECG signal using wavelet transform” , Seena V and Jerrin.Yomas proposes comparison of different feature extraction and denoising techniques using wavelet transform[4].

In the paper “A Survey on ECG Signal DenoisingTechniques”, Sarang L. Joshi, Rambabu A.Vatti and Rupali V.Tornekar show that to remove motion artifact and EMG noise we should select discrete Meyer wavelet and apply the improved thresholding function which combines features of hard and soft thresholding[5] .

In ECG signal analysis QRS detection is very important for diagnosis of patients, through this wave clinical information like heart rate, type of arrhythmic diseases etc can be evaluated. But the detection of QRS is very difficult because it is contaminated by several noises like base line wander, motion artifacts, power line interference etc. Wavelet is efficient tool for signal representation in time and frequency. Wavelet based ECG signal feature extraction and abnormal heart beat reorganization is done by Castro et al [7]. In this method mother wavelet among the orthogonal and bi orthogonal are chosen. For feature extraction signal is de noised and then mother wavelet function is applied to get the features.

The ECG signal amplitude is very small and its frequency range lies between 0.05-100 Hz. This ECG signal is corrupted by several artifacts signals those are power line interference 50/60 Hz, motion artifacts, muscle contraction, baseline drift noise, and Instrumentation

noise due to electronic devices, so characteristics of ECG signal changes and changes the features of ECG signal. Thus removal of such artifacts is very necessary to get correct ECG signal.

In the paper titled, "Optimal selection of wavelet basis function applied to ECG signal denoising", B. N. Singh and A. K. Tiwari have applied an optimal wavelet basis function for denoising of an ECG signal [13]. The experimental results have revealed suitability of Daubechies mother wavelet of order 8 to be the most appropriate wavelet basis function for the denoising application.

Several other techniques have been also proposed to extract the ECG components contaminated with the background noise and allow the measurement of subtle features in the ECG signal.

1.3 Report Layout

The summary of all chapters covered in this dissertation report is as follows:

Chapter 1: The chapter is the introduction to analysis and denoising of ECG signals. Different literature survey for denoising of ECG signal algorithm are briefly discussed.

Chapter 2: This Chapter explains the generation of heart beat, basics of electrocardiogram and ECG morphology. Artifacts that commonly appear in ECG signal during acquisition are elaborately discussed. Different modes of lead placement and the MIT-BIH arrhythmias database are also described.

Chapter 3: This chapter describes wavelet transforms and different approaches which are implemented in this thesis to denoise the ECG signal including signal decomposition, thresholding and signal reconstruction.

Chapter 4: In this chapter the result and discussion of the work carried out from generation of noise to denoising of ECG signal. Comparison of result in terms of various parameter like SNR, PRD and MSE

Chapter 5: Finally in this chapter the conclusion and future scope of the work have been presented.

CHAPTER 2

BASICS OF ECG AND ARTIFACTS

This Chapter explains basics of electrocardiogram, the generation of heart beat and morphology of ECG waveform. Artifacts that commonly appear in ECG signal during acquisition are elaborately discussed. Different modes of lead placement and the MIT-BIH arrhythmia database are also described.

2.1 Electrocardiogram

The ECG is a bioelectric signal, which records the electrical activity of heart versus time. Therefore, it is an important diagnostic tool for assessing heart function. The ECG is acquired by placing electrodes on the skin of the patient. The ECG signal provides the following information of a human heart [15]:

- disturbances in heart rhythm and conduction
- abnormalities in the spread of electrical impulse across the heart
- information about a prior heart attack
- sign of coronary artery disease
- abnormal thickening of heart muscle
- indication of decreased oxygen delivery to the heart
- extent and location of myocardial ischemia
- changes in electrolyte concentrations

• effects of drugs on the heart

2.1.1 Structure and Physiology of Heart

The human heart weighs 250- 350 grams and is approximately equal to the size of the fist. It is located anterior to the vertebral columnπand posterior to the sternum. It is covered by a double-walled sac called the pericardium. The exterior part of this sac is called the fibrous pericardium. This sac protects the heart, anchors its surrounding structures and prevents overfilling of the heart with blood. The outer wall of the human heart is composed of three layers. The outer layer is called the epicardium or visceral pericardium since it is also the inner wall of the pericardium. The middle layer is called the myocardium and is composed of cardiac muscle which contracts. The inner layer is called the endocardium and is in contact with the blood. It also merges with the inner lining (endothelium) of blood vessels and covers heart valves [20].

The Heart is divided into separate right and left sections by the interventricular septum. Each of these (right and left) sections are again divided into upper and lower compartments known as atria and ventricles respectively. Thus, human heart has four chambers i.e. two superior atria and two inferior ventricles. The atria are the receiving chambers and the ventricles are the discharging chambers as shown in the Fig. 2.1. The atria are attached to the ventricles by fibrous, non-conductive tissue that keeps the ventricles electrically isolated from the atria. The Tricuspid valve separates the right atrium from the right ventricle. The Mitral (also known as the Bicuspid) valve separates the left atrium from the left ventricle.

Oxygen-poor blood from the whole body is received into the right atrium through large veins called the superior and inferior vena cava and flows. The right atrium and the right ventricle together form a pump to the circulate blood to the lungs. The right ventricle then pumps the blood to the lungs where the blood is oxygenated. Similarly, the left atrium and the left ventricle together form a pump to circulate oxygen-enriched blood received from the lungs (via the pulmonary veins) to the rest of the body [15].

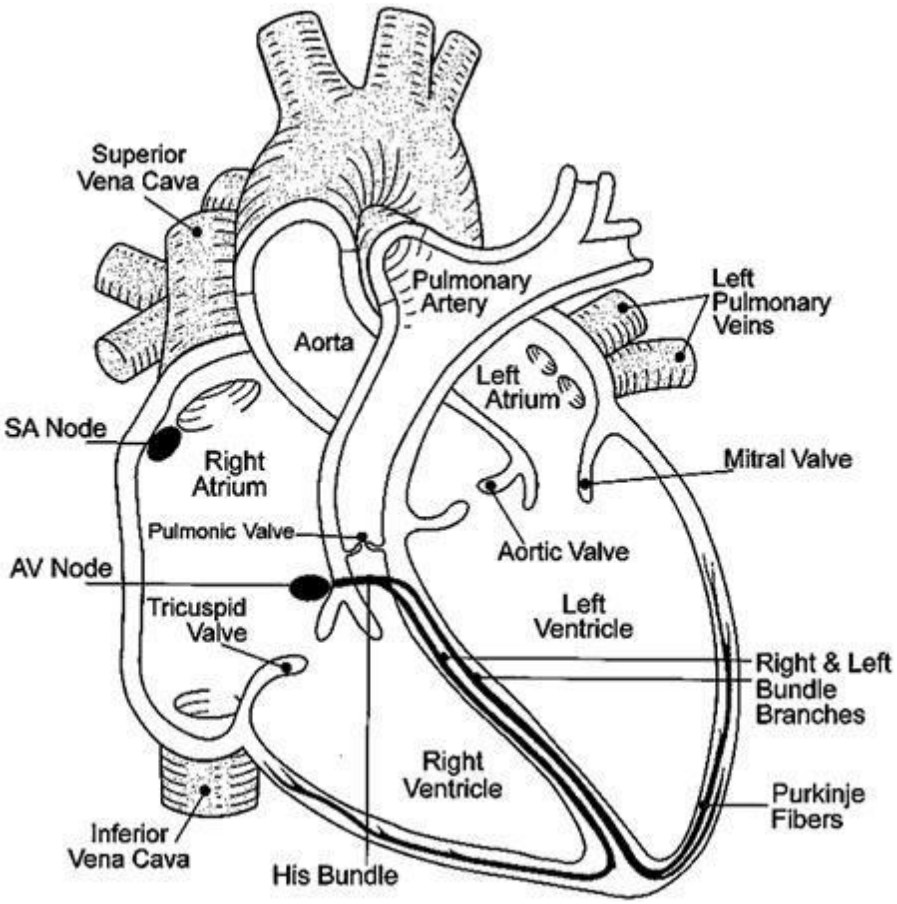

Figure 2.1: Structure of heart

2.2 Generation of Heart Beat

Some cardiac cells are self-excitable, contracting without any signal from the nervous system. Even if removed from the heart and placed in culture, the cells have the self-excitation property. The electrical potentials for contraction are caused by a group of specialized cells in the heart which control the heartbeat. These cells produce electrical impulses which spread across the heart causing it to contract. The main pacemaker of

heart, the Sinoatrial node (SA node), initiates the heart beat by generating an electrical impulse which travels to the left and right atria, causing them to contract (atrial depolarization). Following the start of atrial depolarization, the impulse quickly arrives at the Atrioventricular node (AV node) which is responsible for the contraction of ventricle. The electrical signal next passes through the Bundle of His, diverges into the Right and Left Bundle branches, and spreads through the Purkinje Fibers to the muscles of the left and right ventricle. This causes ventricular depolarization (contraction). The time required for the signal to travel from the AV node to the Purkinje Fibers provides a natural delay of about 0.1 second. This delay ensures that the atria have become completely empty before the ventricles contract. The contraction is followed by ventricular repolarization (recovery) of the cells which were excited during the previous depolarization wave.

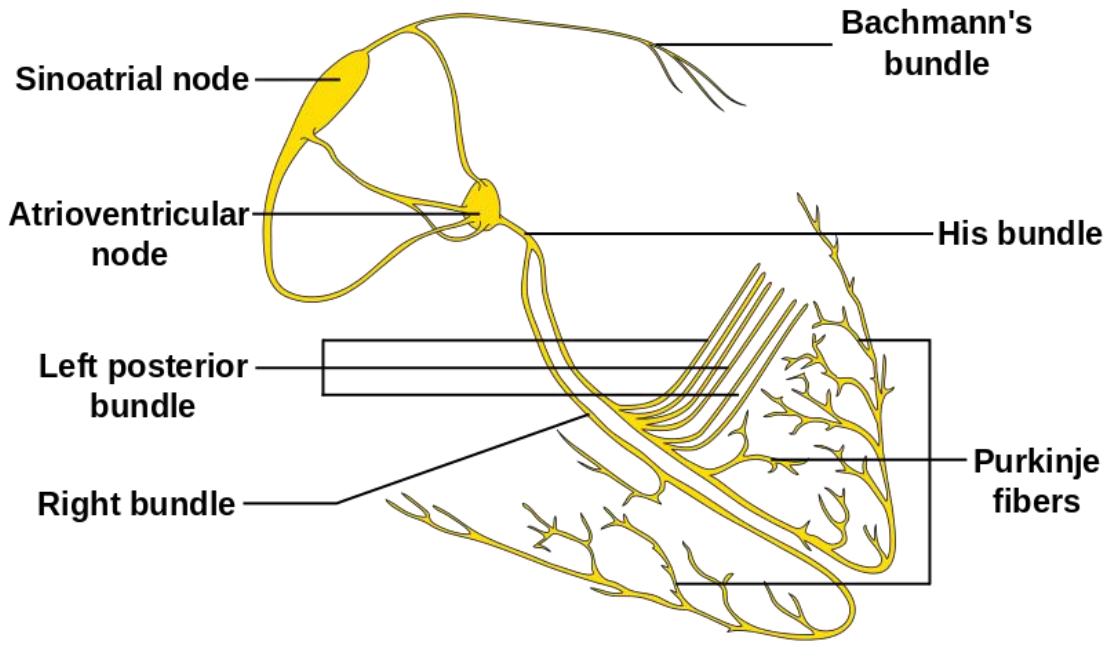

Figure 2.2: Conduction path of electrical potential for heart beat

The SA node creates the electrical impulse which causes the heart to beat, but the Autonomic Nervous System (ANS) controls the heart rate and the strength of heart

contractions. The ANS consists of two parts, the Sympathetic Nervous System (SNS) and the Parasympathetic Nervous System (PNS). The Sympathetic nerves increase the heart rate and the contraction force, while the Parasympathetic nerves act in the reverse manner. An idealized conduction of electrical impulse for heart beat is shown in Fig. 2.2. A small portion of this electrical potential flows to the body surface. By applying electrodes on the skin at the selected points, the electrical potential generated by this current can be recorded as an ECG signal [14].

2.3 ECG Morphology

ECG waveform of a normal individual consists of P wave, QRS complex, ST segment, T wave and U wave. The labels of Fig. 2.3 are commonly used in medical ECG terminology.

P wave: When the electrical impulse is conducted from the SA node towards the AV node and spreads from right to left atrium, the depolarization (contraction) of the atria occurs. The depolarization of atria results the P Wave in the ECG.

QRS complex: The QRS complex consists of three waves, sequentially known as Q, R and S. The rapid depolarization of both the ventricles results this complex. The muscles of the ventricles have large muscle mass than that of atria, hence its amplitude is much larger than that of P wave.

T wave: Ventricular repolarisation results the preceding of ST segment and the T wave.

U wave: The origin of U wave is not clear and it is rarely seen. It is probably produced due to the repolarisation of the papillary muscles.

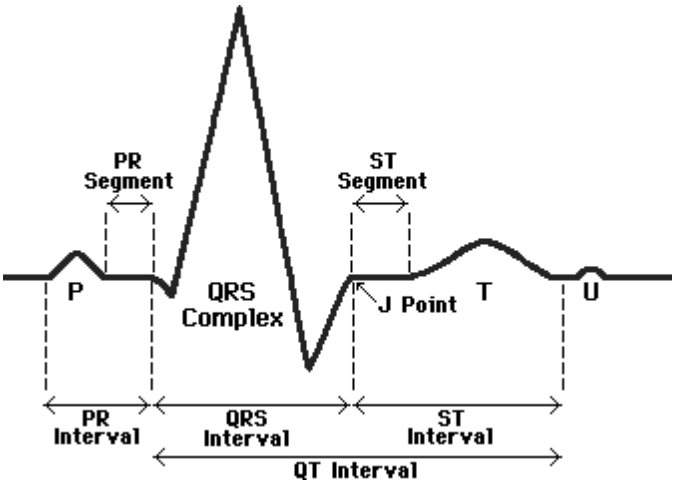

Figure 2.3 ECG waveform

Table 2.1 Features of ECG signal

Features	**Description**	**Amplitude**	**Duration**
P wave	Atrial depolarization	0.1-0.2 mv	80 ms
PR interval	Reflects the time the electrical impulse takes to travel from the sinus node through the AV node and entering the ventricles	_	120-200ms
QRS complex	Depolarization of ventricles	1-1.2 mv	80-120 ms
J point	Point where QRS complex is finished	_	_
ST interval	Represents the period when the ventricles are depolarized	_	80-120 ms
T wave	Repolarisation of ventricles	0.12-0.3mv	160 ms
QT interval	is measured from the beginning of the QRS complex to the end of the T wave. A prolonged QT interval is a risk factor for ventricular tachyarrhythmias and sudden death	_	300-430ms
U wave	repolarisation of the papillary muscles, rarely seen	_	_
RR interval	The interval between an R wave and the next R wave	_	0.2-1.2 s

2.4 Noises in ECG

ECG measurements may be corrupted by many sorts of noise. The ones of primary interest are:

• Power line interference

• Electrode contact noise

• Motion artifacts

• EMG noise

• Instrumentation noise

These artifacts strongly affects the ST segment, degrades the signal quality, frequency resolution, produces large amplitude signals in ECG that can resemble PQRST waveforms and masks tiny features that are important for clinical monitoring and diagnosis. Cancelation of these artifacts in ECG signals is an important task for better diagnosis.

2.4.1 Power Line Interference

Power line interference occurs through two mechanisms: capacitive and inductive coupling. Capacitive coupling refers to the transfer of energy between two circuits by means of a coupling capacitance present between the two circuits. The value of the coupling capacitance decreases with increasing separation of the circuits. Inductive coupling on the other hand is caused by mutual inductance between two conductors. When current flows through wires it produces a magnetic flux, which can induce a current in adjacent circuits. The geometry of the conductors as well as the separation between them determines the value of the mutual inductance, and hence the degree of the inductive coupling. Typically, capacitive coupling is responsible for high frequency noise while inductive coupling

introduces low frequency noise. For this reason inductive coupling is the dominant mechanism of power line interference in electro cardiology. To limit the amount of power line interference, electrodes should be applied properly, that there are no loose wires, and all components have adequate shielding.

The Power line interference has frequency of 60 Hz or 50 Hz depending on the power supply.

2.4.2 Electrode Contact Noise

Electrode contact noise is caused by variations in the position of the heart with respect to the electrodes and changes in the propagation medium between the heart and the electrodes. This causes sudden changes in the amplitude of the ECG signal, as well as low frequency baseline shifts. In addition, poor conductivity between the electrodes and the skin reduces the amplitude of the ECG signal and increases the probability of disturbances (by reducing SNR).

The underlying mechanism resulting in these baseline disturbances is electrode-skin impedance variation. The larger the electrode-skin impedance, the smaller the relative impedance change needed to cause a major shift in the baseline of the ECG signal. If the skin impedance is extraordinarily high, it may be impossible to detect the signal features reliably in the presence of body movement. Sudden changes in the skin-electrode impedance induce sharp baseline transients which decay exponentially to the baseline value. This transition may occur only once or rapidly several times in succession. Characteristics of this noise signal include the amplitude of the initial transition and the time constant of the decay.

2.4.3 Motion Artifacts

Motion artifacts are baseline changes caused by electrode motion. The usual causes of motion artifacts are vibrations, movement, or respiration of the subject. The peak amplitude and duration of the artifacts are random variables which depend on the variety of unknowns such as the electrode properties, electrolyte properties (if one is used between the electrode and skin), skin impedance, and the movement of the patient. In this ECG signal, the baseline drift occurs at an unusually low frequency (approximately less than 1Hz).

2.4.4 Electromyographic Noise

Electromyographic noise is caused by the contraction of other muscles besides the heart. When other muscles in the vicinity of the electrodes contract, they generate depolarization and repolarization waves that can also be picked up by the ECG. The extent of the crosstalk depends on the amount of muscular contraction (subject movement), and the quality of the probes. It is well established that the amplitude of the Electromyographic signal is stochastic (random) in nature and can be reasonably modelled by a Gaussian distribution function. The mean of the noise can be assumed to be zero; however, the variance is dependent on the environmental variables and will change depending on the conditions. Certain studies have shown that the standard deviation of the noise is typically 10% of the peak-to-peak ECG amplitude. While the actual statistical model is unknown, it should be noted that the electrical activity of muscles during periods of contraction can generate surface potentials comparable to those from the heart and could completely drown out the desired signal. The frequency of this EMG noise is in between 100-500 Hz.

2.4.5 Instrumentation Noise

The electrical equipment's used in ECG measurements also contribute noise. The major sources of this form of noise are the electrode probes, cables, signal processor or

amplifier, and the analog-to-digital converter. Unfortunately instrumentation noise cannot be eliminated as it is inherent in electronic components, but it can be reduced through higher quality equipment and careful circuit design. Another form of noise, called flicker noise, is very important in ECG measurements, due to the low frequency content of ECG data. The actual mechanism that causes this type of noise is not yet understood, but one widely accepted theory is that it is caused by the energy traps which occur between the interfaces of two materials. It is believed that the charge carriers get randomly trapped/released and cause flicker noise.

2.5 ECG Database

Since 1975, the laboratories at Boston's Beth Israel Hospital (now the Beth Israel Deaconess Medical Centre) and at Massachusetts Institute of Technology (MIT) have supported the research in arrhythmia analysis and related subjects by creating a database. One of the first major products of their effort was the Massachusetts Institute of Technology Beth Israel Hospital (MIT-BIH) database. This database was completed and began distributing in 1980. The database was the first generally available set of standard test material for evaluation of arrhythmia detectors and has been used for that purpose as well as for basic research into cardiac dynamics at more than 500 sites worldwide [26].

The MIT-BIH Arrhythmia Database contains 48 half-hour excerpts of two-channel ambulatory ECG recordings. These are obtained from 47 subjects collected from a mixed population of inpatients (about 60%) and outpatients (about 40%) studied by the BIH Arrhythmia Laboratory. The subjects were taken from, 25 men aged 32 to 89 years and 22 women aged 23 to 89 years. About half (25 of 48 complete records and reference annotation files for all 48 records) of this database has been freely available in PhysioNet's inception in September 1999 [8]. The 23 remaining signal files, which had been available only on the MIT-BIH Arrhythmia Database CD-ROM, were posted in

February 2005. The recordings were digitized at 360 samples per second per channel with 11-bit resolution over a 10 mV range.

CHAPTER 3

WAVELETS AND ECG DENOISING ALGORITHMS

Algorithms which are implemented in this thesis for ECG enhancement purpose are described here. For denoising purpose thresholding and wavelet filter bank are used.

3.1 Wavelet Transform

The Fourier transform is useful tool to analyze the frequency components of the signal. However, if we take the Fourier transform over the whole time axis, we cannot tell at what instant a particular frequency rises. Short-time Fourier transform (STFT) uses a sliding window to find spectrogram, which gives the information of both time and frequency. But still another problem exists i.e. the length of window limits the resolution in frequency. Wavelet transform seems to be a solution to the problem above. Wavelet transforms (WT) are based on small wavelets with limited duration. In WT both the time and frequency resolutions vary in time-frequency plane in order to obtain a multiresolution analysis.

In wavelet transform, a signal *x(t)* which belongs to the square integrable subspace L2(R) is expressed in terms of scaling function $\varphi_{j,k}(t)$ and mother wavelet function $\psi_{j,k}(t)$. Here *j* is the parameter of dilation or the visibility in frequency and *k* is the parameter of the position.

$$x(t)=\sum_{k} a_{j_0,k}\,\varphi_{j_0,k}(t)+\sum_{j=j_0}^{\infty}\sum_{k} b_{j,k}\,\psi_{j,k}(t)$$

where a, b are the coefficients associated with $\varphi_{j,k}(t)$ and $\psi_{j,k}(t)$ respectively.

The coefficients a, b can be calculated as we calculate the coefficients in Fourier transform.

The expression of a, b are given in the following equations

$$a_{j_0,k} = \int_{-\infty}^{\infty} x(t)\,\varphi_{j_0,k}(t)\,dt$$

$$b_{j,k} = \int_{-\infty}^{\infty} x(t)\,\psi_{j,k}(t)\,dt$$

The scaling function $\varphi_{j,k}(t)$ can be expressed as

$$\varphi_{j,k}(t) = 2^{j/2}\,\varphi\left(2^j t - k\right)$$

$\psi_{j,k}(t)$ can also be derived from its shifted version i.e. $\varphi_{j,k}(2t)$. The expression of $\varphi_{j,k}(t)$ in terms of $\varphi_{j,k}(2t)$ will be

$$\varphi(t) = \sum_n h_\varphi(n)\sqrt{2}\,\varphi(2t-n)$$

n is the shifting parameter and $h_\varphi(n)$ are the coefficients.

The mother wavelet function $\psi_{j,k}(t)$ is expressed as

$$\psi_{j,k}(t) = 2^{j/2}\,\psi\left(2^j t - k\right)$$

$\psi_{j,k}(t)$ can also be written using shifted version $\varphi_{j,k}(t)$ i.e. $\varphi_{j,k}(2t)$.

The expression of $\psi_{j,k}(t)$ will be

$$\psi(t)=\sum_{n} h_{\psi}(n)\sqrt{2}\,\varphi(2t-n)$$

n is the shifting parameter and $h_{\psi}(n)$ are the coefficients.

3.2 Discrete Wavelet Transform

The discrete wavelet transform (DWT) is an implementation of the wavelet transform using a discrete set of the wavelet scales and translations obeying some defined rules. In other words, this transform decomposes the signal into mutually orthogonal set of wavelets.

The scaling function $\varphi_{j,k}(n)$ and the mother wavelet function $\psi_{j,k}(n)$ in discrete domain are

$$\varphi_{j,k}(n)=2^{j/2}\,\varphi\left(2^{j}n-k\right)$$

$$\psi_{j,k}(n)=2^{j/2}\,\psi\left(2^{j}n-k\right)$$

The DWT of an discrete signal x(n) of length M-1 is given by

$$x(n)=\sum_{k} W_{\varphi}(j_0,k)\,\varphi_{j_0,k}(n)+\sum_{j=j_0}^{\infty}\sum_{k} W_{\psi}(j_0,k)\,\psi_{j,k}(n)$$

Here, $W\varphi(j_0,k)$ and $W\psi(j_0,k)$ are called the wavelet coefficients.

$\varphi_{j,k}(n)$ and $\psi_{j,k}(n)$ are orthogonal to each other. Hence we can simply take the inner product to obtain the wavelet coefficients.

$$W_{\varphi}[j_0,k]=\frac{1}{\sqrt{M}}\sum_{n}x(n)\varphi_{j_0,k}[n]$$

$$W_{\psi}[j,k]=\frac{1}{\sqrt{M}}\sum_{n}x(n)\psi_{j_0,k}[n] \quad j\geq j_0$$

The coefficients $W\varphi(j_0,k)$ are called the approximation coefficients and the coefficients $W\psi(j_0,k)$ are called the detailed coefficients. The DWT can be realized in terms of high pass and low pass filters. The approximation properties of filter banks and their relation to wavelets are presented in the paper [44]. The output of the low pass filter gives the approximation coefficients and the output of the high pass filter gives the detailed coefficients. To get the filter coefficients $W\varphi(j_0,k)$ and $W\psi(j_0,k)$ can be rewritten as

$$W_{\varphi}(j,k)=\sum_{n}h_{\varphi}(n-2k)W_{\varphi}(j+1,m)$$

$$W_{\psi}(j,k)=\sum_{m}h_{\psi}(m-2k)W_{\psi}(j+1,m)$$

h_{φ} and h_{ψ} are the filter coefficients of the low pass filter and high pass filter respectively.

Computation of the wavelet coefficients at every possible scale is a fair amount of work and it generates an awful lot of data. Selection of a subset of scales and positions based on powers of two (dyadic scales and positions) results in a more efficient and accurate analysis. Mallat has introduced repetitive application of high pass and low pass filters to calculate the wavelet expansion of a given sequence of discrete numbers [14].

3.3 Wavelet Decomposition

The DWT decomposes the signal into approximate and detail information as discussed in section 3.2. Thus, it helps in analyzing the signal at different frequency bands with different resolutions.

3.3.1 Single stage wavelet filtering

In single stage wavelet filtering the original signal *x(n)* is passed through two complementary filters and emerges as two signals. The filtering process, at its most basic level is shown in Fig. 3.1.

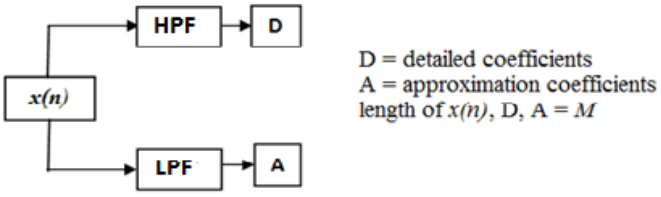

Figure 3.1 Single stage wavelet filtering

If single stage wavelet filter is applied on a digital signal, then we end with twice as much data as we started with. The original signal x(n) consists of M samples of data. The resulting approximation and detail coefficients are each of length M, for a total of 2M.

There exists an alternative method to perform the decomposition using wavelets. By down sampling A and D to half of their lengths i.e. M/2, the total length of resulting signal can be maintained. The final output signals after down sampling are denoted as cA and cD. It is diagrammatically shown in Fig. 3.2.

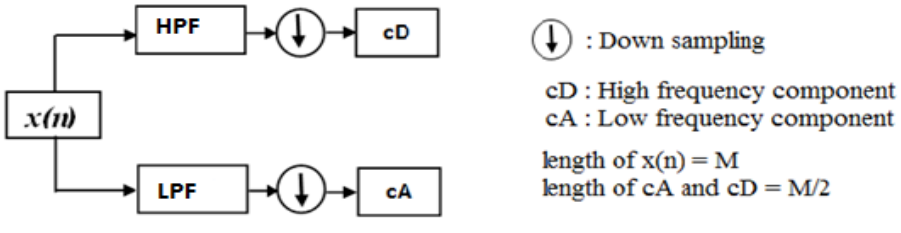

Figure 3.2 Single stage wavelet filtering with down sampling

3.3.2 Multistage wavelet filtering

The wavelet decomposition process can be iterated, so that one signal is broken down into many lower resolution components. This is called the wavelet decomposition tree.

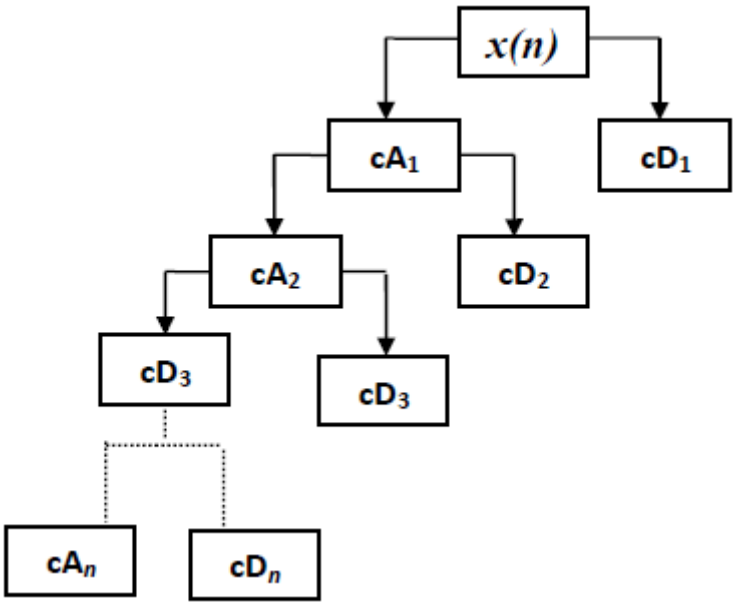

Figure 3.3 Multistage wavelet decomposition tree

Since multistage wavelet filtering analysis process is iterative, theoretically it can be continued till infinite levels. Ideally the decomposition can be done only until the individual details consist of a single sample. In practice, a suitable number of decomposition levels based on the nature and frequency component of the signal.

3.4 Thresholding

3.4.1 Soft of Hard Thresholding

Thresholding can be either soft or hard . Hard thresholding zeroes out all the signal values smaller than Y. Soft thresholding does the same thing, and apart form that, subtracts Y from the values larger than Y. In contrast to hard thresholding, soft thresholding causes no discontinuities in the resulting signal. In Matlab, by default, soft thresholding is used for denoising and hard thresholding for compression. There are two ways to apply the threshold value to the wavelets coefficients; the hard and soft thresholds which were expressed as formulas respectively as shown in Figure 3.5

$$Y = \begin{cases} 0 & |Y| < Thr \\ Y & |Y| \geq Thr \end{cases}$$

$$Y = \begin{cases} 0 & |Y| < Thr \\ sign(Y) * (|Y| - Thr) & |Y| \geq Thr \end{cases}$$

Y is the wavelets coefficient.

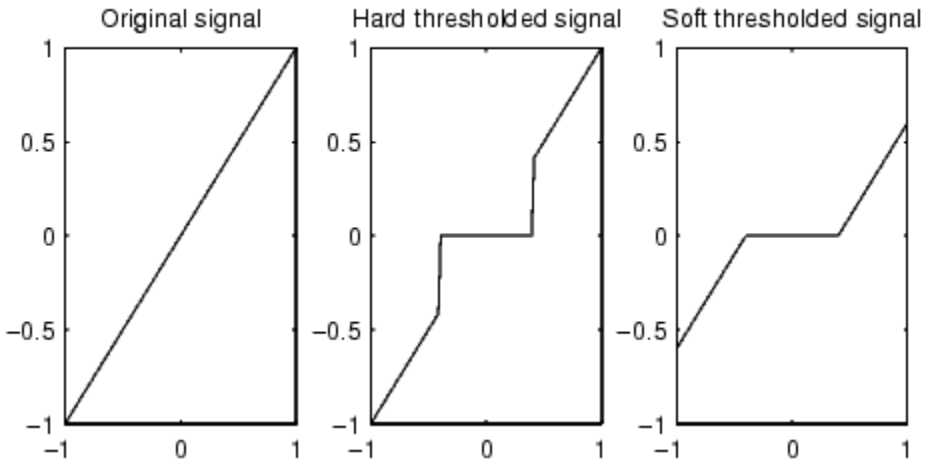

Fig. 3.4 Hard and Soft Thresholding

3.4.2 Selection of Threshold

Thresholding of the wavelet coefficients can be done using either hard thresholding or soft thresholding [14]. The selection of the threshold value for denoising can be done using any of the four selection rules explained as below [7]:

MINMAX Thresholding: It uses a fixed threshold chosen to yield minimax performance for mean square error against an ideal procedure. The minimax principle is used in statistics in order to design estimators. Since the de-noised signal can be assimilated to the estimator of the unknown regression function, the minimax estimator is the one that realizes the minimum of the maximum mean square error obtained for the worst function in a given set.

RIGEROUS SURE Thresholding: It is used for the soft threshold estimator based on Stein's Unbiased Estimate of Risk (quadratic loss function). One gets an estimate of the risk for a particular threshold value and minimizing the risks and gives a selection of the threshold value.

UNIVERSAL Thresholding: This was proposed by Donoho and can be used as an alternative to the use of minimax threshold. It is bigger in magnitude than the minimax threshold. The value of the threshold is calculated as:

THR = sqrt (2*log(length(X))

Where, THR is the threshold value and X is noisy signal.

HEURISTIC SURE Thresholding: This is a heuristic variant of the rigorous sure method. It is a mixture of the two previous options. As a result, if the signal to noise ratio is very small, the SURE estimate is very noisy. If such a situation is detected, the fixed form threshold is used.

3.5 Wavelet Reconstruction

In section 3.2.3, the analysis of a signal by discrete wavelet transform decomposition is discussed. This process is called decomposition or analysis. After decomposition, the task is to again reconstruct the original signal without loss of important information. This process is called reconstruction, or synthesis. The synthesis is done mathematically by using the inverse discrete wavelet transform (IDWT).

In wavelet analysis, filtering and followed by down sampling are involved. But the wavelet reconstruction process consists of up sampling followed by filtering. Up sampling is the process of lengthening a signal component by inserting zeros between samples.

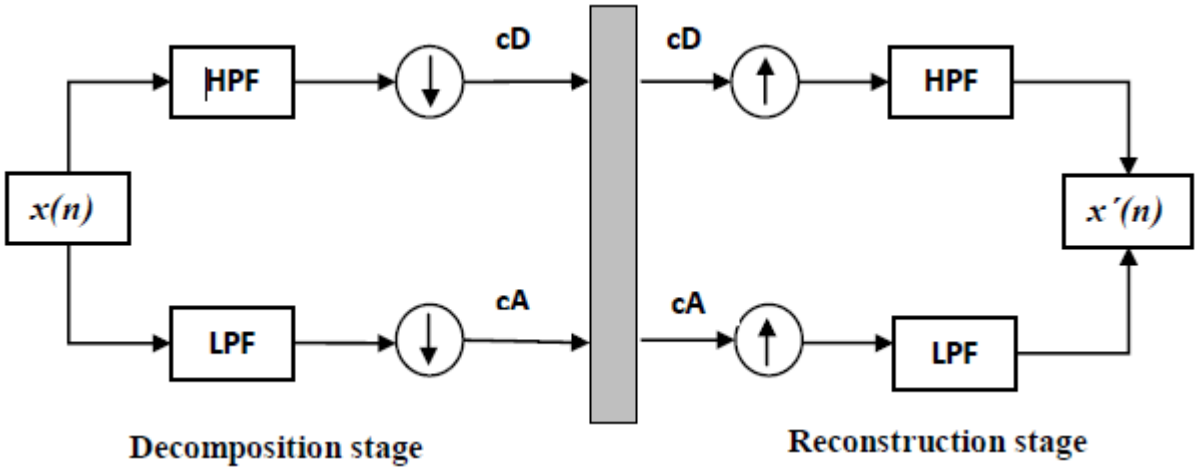

Figure 3.5 Single stage decomposition and reconstruction

We combine cA and cD by IDWT to get the reconstructed original signal. However, instead of combining, we can feed a vector of zeros in place of the detail coefficients vector or approximation coefficients as per our requirement. For example, when cD is made zero before combining with cA, it yields a reconstructed *approximation* A1. A1 has the same length as the original signal *x(n)* and which is a real approximation of it.

For multiple level reconstruction, the single stage reconstruction technique is iterated to reassemble the original signal.

3.6 Denoising Algorithm

- Generation of Noise
- Addition of Noise to Original ECG Signal
- Decomposition of Noisy ECG Signal
- Thresholding
- Reconstruction of ECG Signal
- Performance Evaluation of Denoised ECG Signal

CHAPTER 4

RESULTS AND DISCUSSION

In this chapter, all the simulation results using the algorithms discussed in chapter 3 are presented under different subsections. The ECG waveform taken from MIT-BIH database, generated noises and the corrupted ECG signal are also shown.

4.1 ECG Waveform

All the simulations shown in later parts of thesis are carried out with data no. 103 of MIT-BIH arrhythmia database [8]. The ECG signal waveform is shown in Figure. 4.1

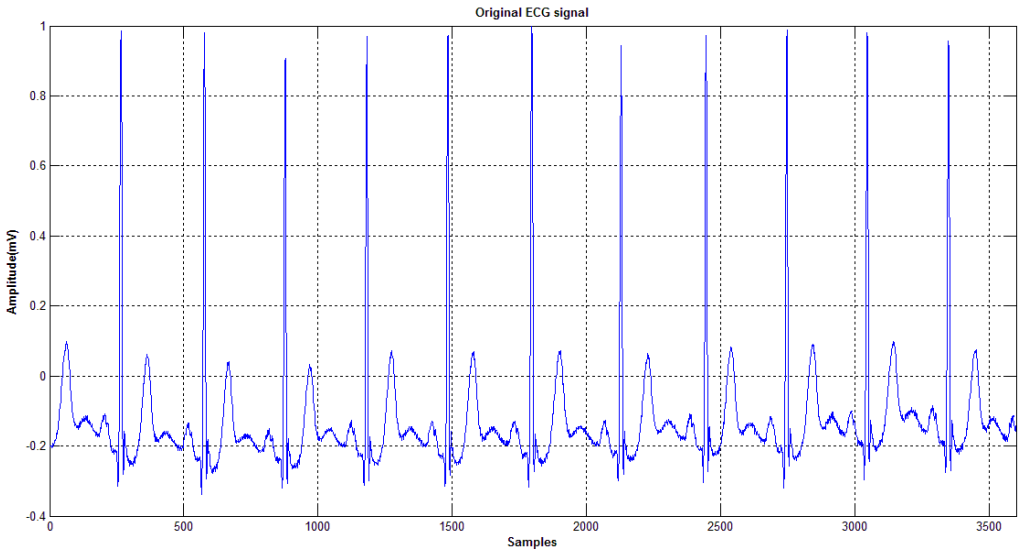

Figure 4.1 ECG Signal from MITBIH arrhythmia database

4.2 Generation of Noise

The artifacts in ECG can be categorized according to their frequency content. The low frequency noise (electrode contact noise and motion artifact) has frequency less than 1 Hz, high frequency noise (EMG noise) whose frequency is more than 100 Hz and power line interference of frequency 50 Hz or 60 Hz (depending on the supply). These noises are generated in MATLAB based on their frequency content.

4.2.1 Generation of Low Frequency Noise

Baseline drift noise is generated by adding two sine waves of frequency 0.4Hz and 0.1Hz and Sawtooth wave of 0.25Hz which is shown in Figure. 4.2.

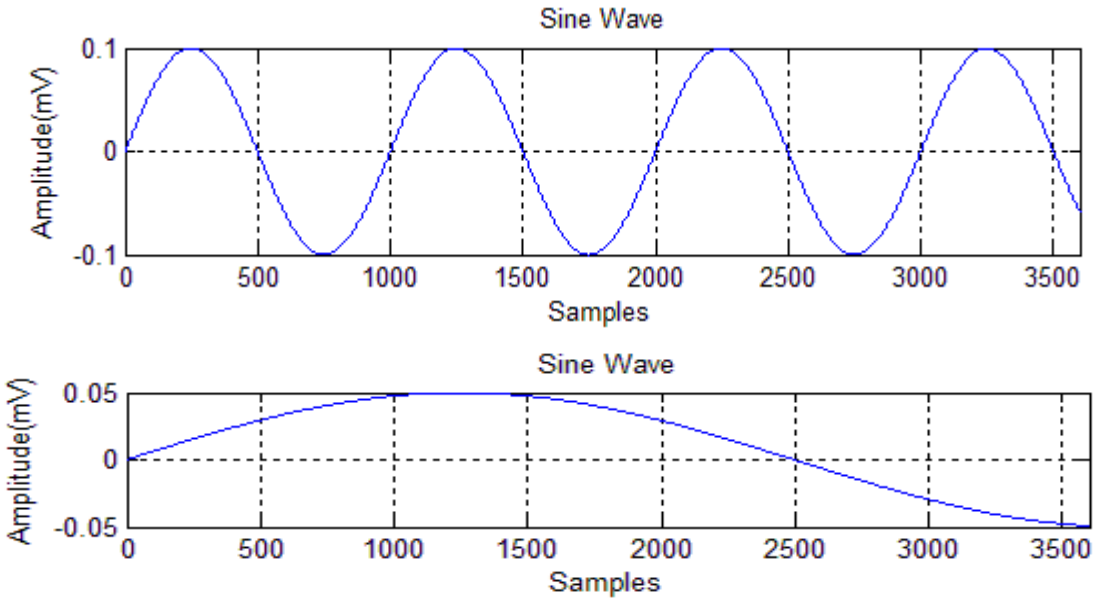

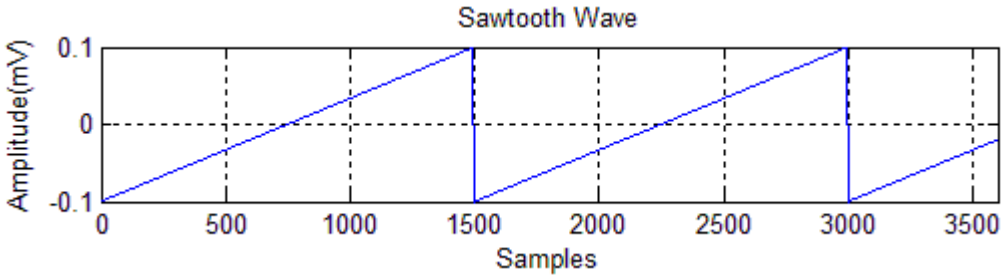

Fig 4.2 Noise Signal of Low Frequency

4.2.2 Generation of High Frequency Noise

High frequency noises are generated by multiplying the sine wave of frequency 150Hz with a random signal. The resulted high frequency noise is shown in Figure. 4.3.

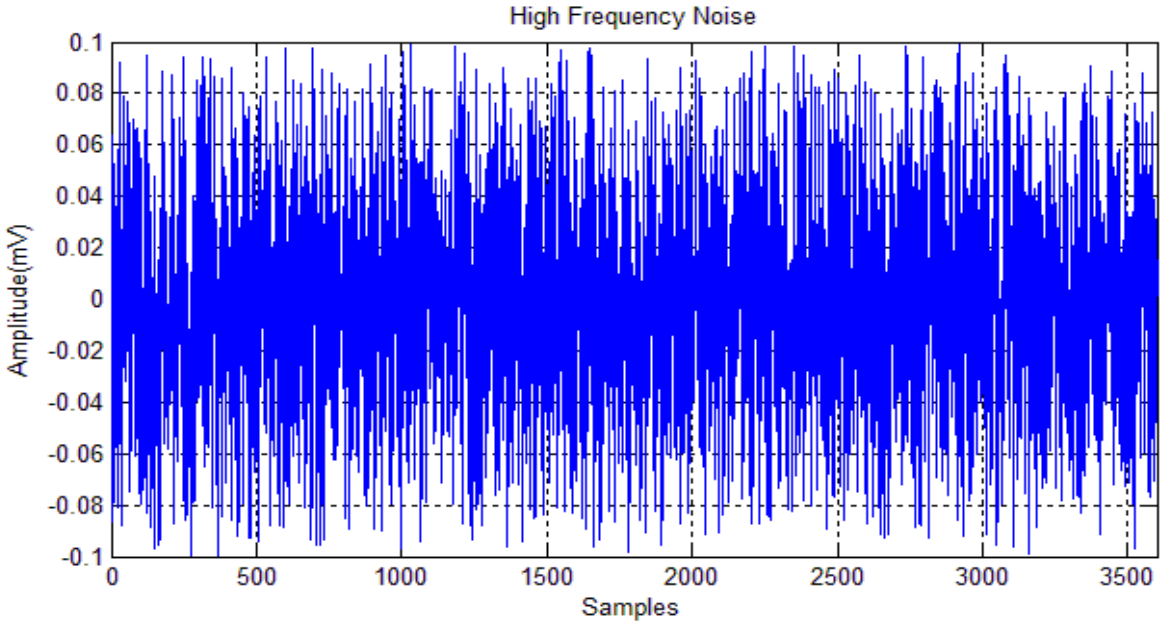

Figure 4.3 High frequency noise

4.2.3 Generation of Power Line Interference

Here the 50Hz power supply is considered. Thus, a sine wave of 50Hz amplitude is taken to represent the power line interference. The generated power line interference is shown in Figure. 4.4.

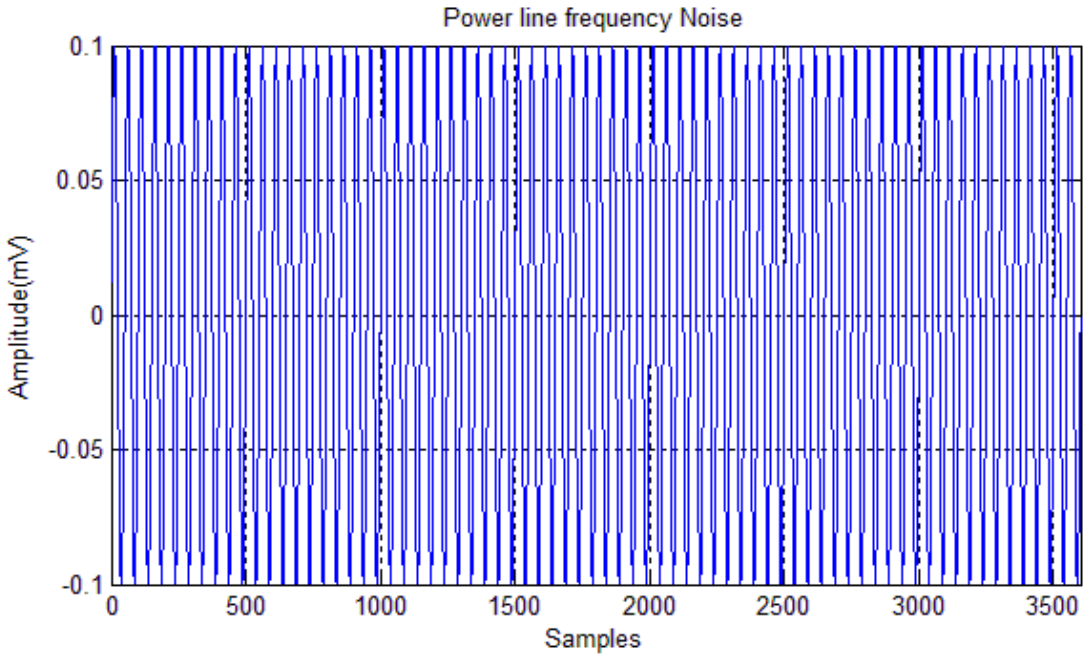

Figure 4.4 Power line interference

4.3 ADDITION OF NOISE TO ECG

The noise signal is generated and are added to form a noise for ECG signals. Now this noise is added with the ECG signals to get the corrupted ECG signal. Figure. 4.5 and Figure. 4.6 shows Noise and the corrupted ECG signal respectively.

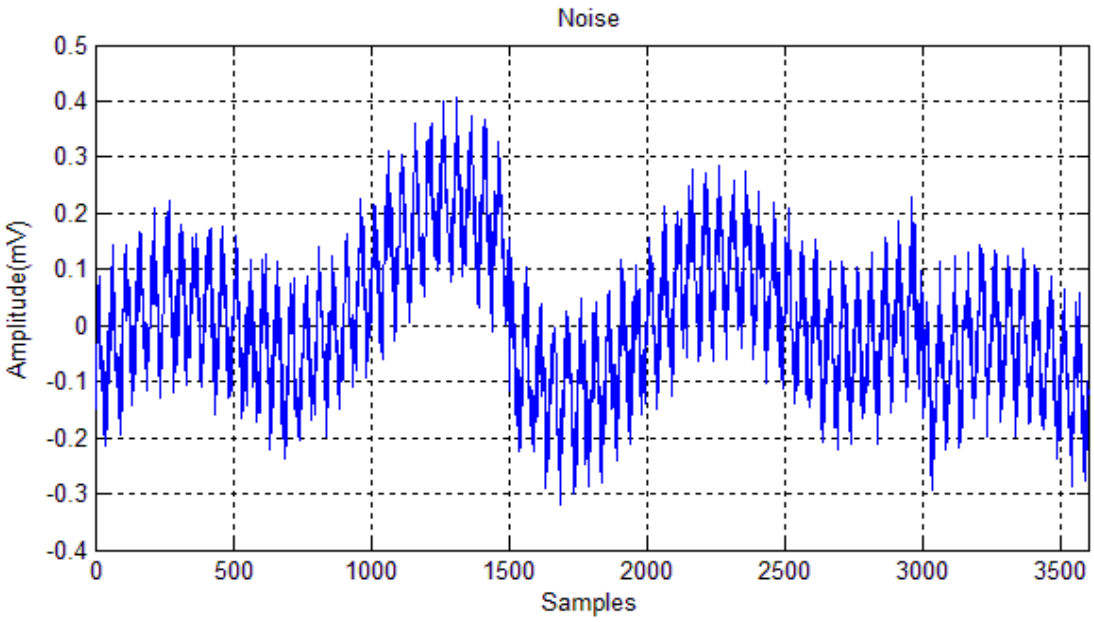

Fig. 4.5 Noise

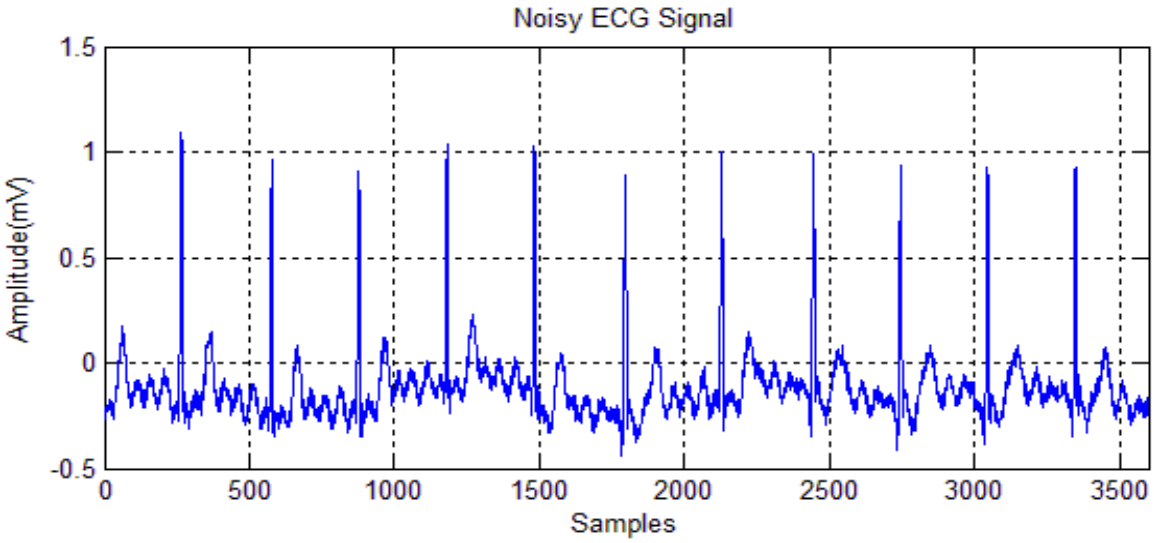

Fig. 4.6 Noisy ECG Signal

4.4 Evaluation Factor of Denoising

For evaluation of denoising algorithm following parameters are evaluated.

(a) Percentage Root Mean Square Difference: represents the standard deviation of difference between original signal sample and reconstructed signal. It is represented by equation (4.2).

$$\mathbf{PRD}(\%) = \mathbf{100} * \sqrt{\left(\sum_{\mathbf{n=1}}^{\mathbf{N}} [\mathbf{X(n)} - \mathbf{Y(n)}]^{\mathbf{2}} \middle| \sum_{\mathbf{n=1}}^{\mathbf{N}} [\mathbf{X(n)}]^{\mathbf{2}} \right)} \qquad \textbf{(4.2)}$$

Where X is original signal and Y is reconstructed signal

(b) Signal to Noise Ratio: is the ratio of signal power to noise power which is expressed in decibels (dB). SNR is represented by equation (4.3)

$$\mathbf{SNR} = \mathbf{10} * \mathbf{log_{10}} \left(\sum_{\boldsymbol{n=1}}^{\boldsymbol{N}} [\mathbf{X(n)}]^{\mathbf{2}} \middle| \sum_{\boldsymbol{n=1}}^{\boldsymbol{N}} [\mathbf{X(n)} - \mathbf{Y(n)}]^{\mathbf{2}} \right) \qquad \textbf{(4.3)}$$

(c) Mean Square Error: It measures the average of the squares of the errors or deviations, that is, the difference between the estimator and what is estimated. MSE is a risk function, corresponding to the expected value of the squared error loss or quadratic loss.

$$\boldsymbol{MSE} = 1/N \sum_{\boldsymbol{n=1}}^{\boldsymbol{N}} [\boldsymbol{X(n)} - \boldsymbol{Y(n)}]^{\mathbf{2}}$$

4.5 Results

Table 4.1 ECG analysis of Biorthogonal Mother Wavelet

Biorthogonal	Soft Thresholding			Hard Thresholding		
	PRD	SNR	MSE	PRD	SNR	MSE
1.1	0.3976	8.0109	0.0052	0.3265	9.7232	0.0045
1.3	0.3473	9.185	0.0043	0.2959	10.5769	0.0038
1.5	0.3507	9.101	0.0044	0.2895	10.7657	0.0037
2.2	0.3975	8.0142	0.0056	0.3182	9.9473	0.0043
2.4	0.4288	7.3559	0.0063	0.2935	10.6479	0.0037
2.6	0.3552	8.99	0.0045	0.28	11.0568	0.0034
2.8	0.2868	10.8486	0.0032	0.2698	11.3778	0.0032
3.1	0.7842	2.1116	0.0405	0.6346	3.9502	0.0222
3.3	0.529	5.5306	0.0101	0.4309	7.3123	0.0086
3.5	0.384	8.3134	0.0055	0.3125	10.1038	0.0042
3.7	0.2742	11.2399	0.0031	0.2765	11.1661	0.0033
3.9	0.267	11.4689	0.0029	0.2709	11.3441	0.0032
4.4	0.3782	8.4446	0.005	0.2901	10.7479	0.0036
5.5	0.3899	8.1812	0.0053	0.2831	10.961	0.0035
6.8	0.2993	10.4784	0.0035	0.2734	11.2642	0.0032

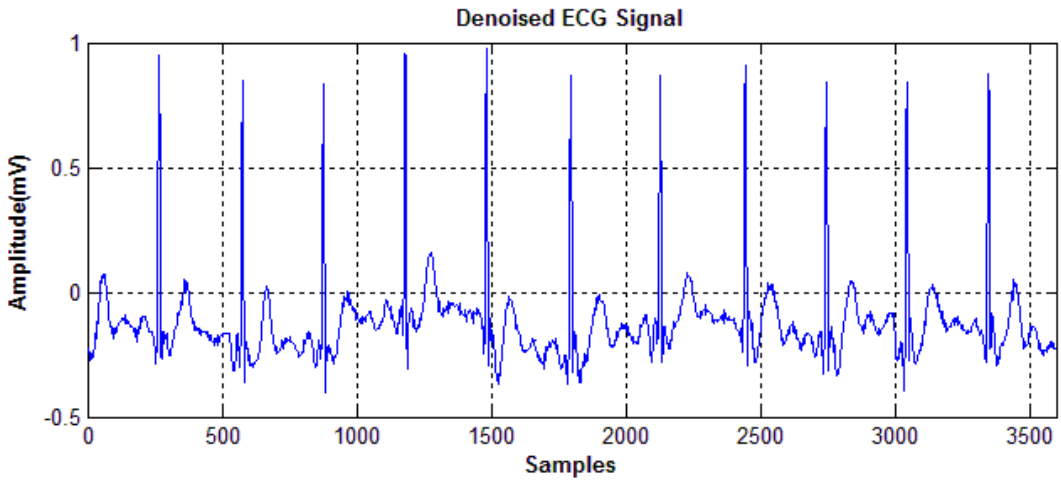

Fig 4.7 Biorthogonal 3.9 wavelet using Soft Thresholding

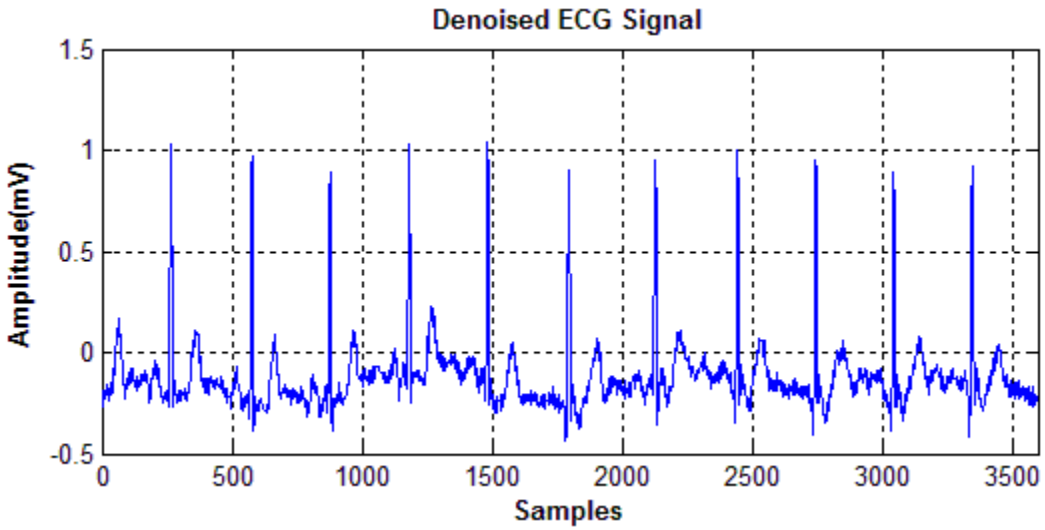

Fig 4.8 Biorthogonal 2.8 wavelet using Hard Thresholding

Table 4.2 ECG analysis of Reverse Biorthogonal Mother Wavelet

Reverse Biorthogonal	Soft Thresholding			Hard Thresholding		
	PRD	SNR	MSE	PRD	SNR	MSE
1.1	0.3992	7.9758	0.0053	0.3228	9.8223	0.0044
1.3	0.3597	8.8805	0.0045	0.2971	10.5416	0.0038
1.5	0.3357	9.4816	0.0041	0.2841	10.9303	0.0035
2.2	0.4756	6.4557	0.0078	0.4025	7.9039	0.0069
2.4	0.4172	7.5933	0.006	0.3282	9.678	0.0047
2.6	0.3794	8.4183	0.0051	0.2916	10.7041	0.0037
2.8	0.3355	9.4863	0.0044	0.2896	10.7653	0.0037
3.1	0.9903	0.0851	0.8908	0.9861	0.1219	0.9092
3.3	0.4592	6.7595	0.0084	0.474	6.485	0.0115
3.5	0.3994	7.9717	0.0061	0.3813	8.375	0.0071
3.7	0.3532	9.0402	0.0049	0.3531	9.0428	0.0058
3.9	0.3304	9.6198	0.0043	0.323	9.8168	0.0047
4.4	0.3597	8.8816	0.0046	0.2787	11.0971	0.0034
5.5	0.4092	7.7619	0.0057	0.2972	10.5376	0.0038
6.8	0.3212	9.8633	0.004	0.2785	11.103	0.0034

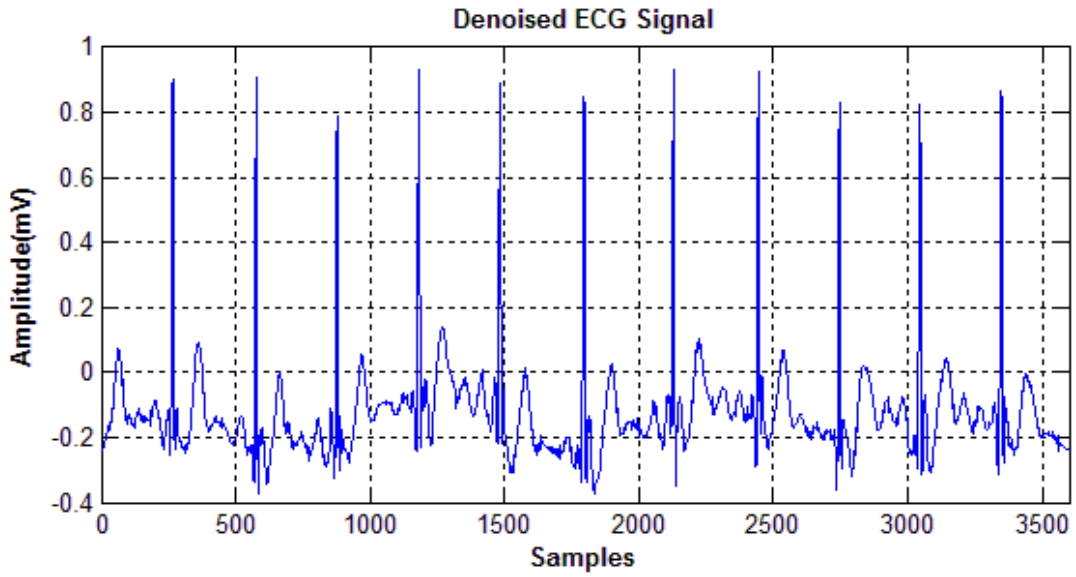

Fig 4.9 Reverse Biorthogonal 6.8 wavelet using Soft Thresholding

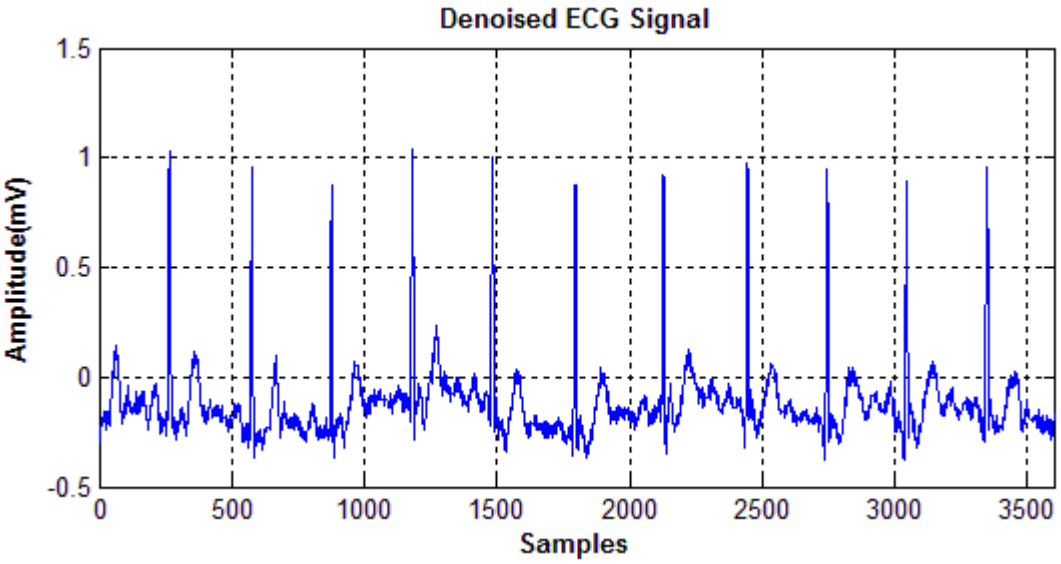

Fig 4.10 Reverse Biorthogonal 6.8 wavelet using Hard Thresholding

Table 4.2 ECG analysis of Symlet Mother Wavelet

Symlet	Soft Thresholding			Hard Thresholding		
	PRD	SNR	MSE	PRD	SNR	MSE
1	0.395	8.0688	0.0052	0.3274	9.6993	0.0045
2	0.4137	7.6665	0.0057	0.3403	9.3621	0.0049
3	0.526	5.5798	0.0087	0.5412	5.3328	0.0104
4	0.4992	6.035	0.0079	0.3648	8.7599	0.0054
5	0.376	8.4957	0.0049	0.2876	10.8233	0.0035
6	0.3637	8.7844	0.0046	0.2786	11.1004	0.0033
7	0.3351	9.4967	0.0041	0.2806	11.0386	0.0034
8	0.3248	9.7673	0.0041	0.2715	11.324	0.0031
9	0.3327	9.5589	0.0043	0.2792	11.0822	0.0034
10	0.3183	9.9437	0.0039	0.2784	11.1066	0.0033
12	0.3032	10.3654	0.0036	0.2796	11.0701	0.0034
15	0.2847	10.9129	0.0035	0.2888	10.7867	0.0037
20	0.2843	10.9257	0.0035	0.286	10.8723	0.0036
25	0.2902	10.7474	0.0036	0.2796	11.0701	0.0034

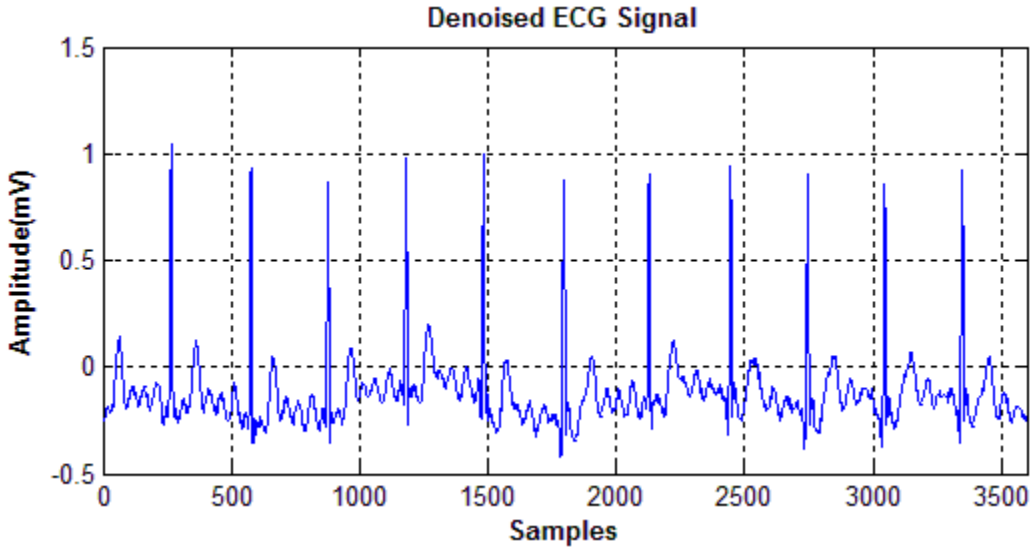

Fig 4.11 Symlet 20 wavelet using Soft Thresholding

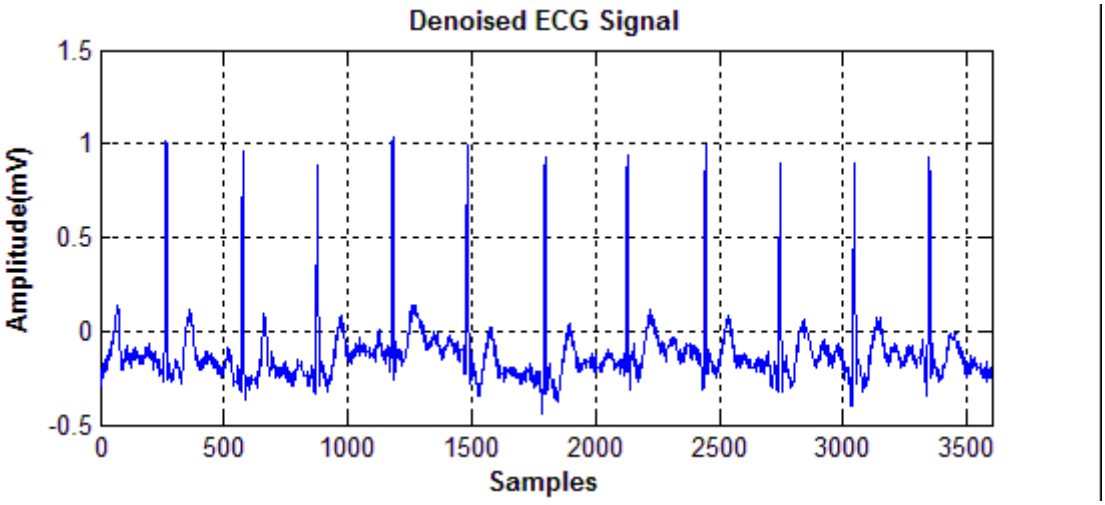

Fig 4.12 Symlet 8 wavelet using Hard Thresholding

Table 4.4 ECG analysis of Coiflet Mother Wavelet

Coiflet	Soft Thresholding			Hard Thresholding		
	PRD	SNR	MSE	PRD	SNR	MSE
1	0.4742	6.4811	0.0074	0.3741	8.5393	0.0057
2	0.3405	9.3566	0.0041	0.2946	10.6145	0.0037
3	0.3007	10.4384	0.0035	0.2708	11.3455	0.0032
4	0.2937	10.6426	0.0034	0.2685	11.4207	0.0031
5	0.2838	10.9404	0.0035	0.2861	10.8697	0.0036

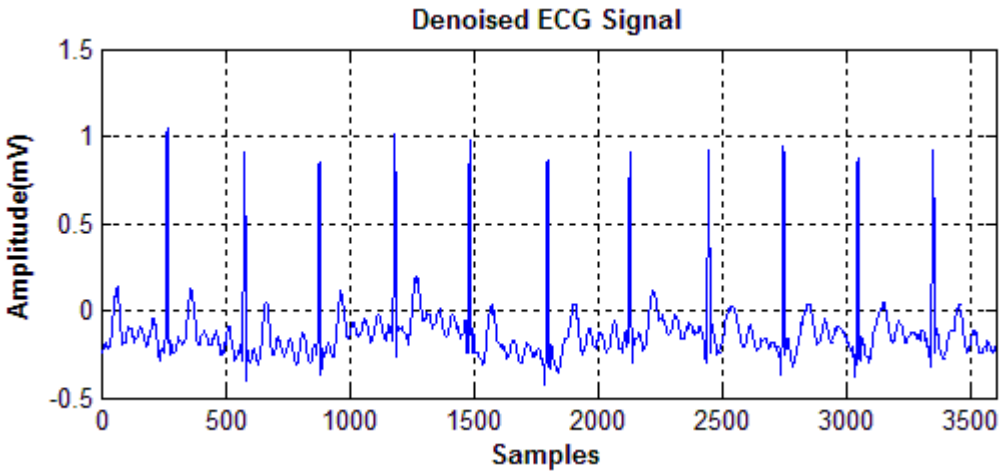

Fig 4.13 Coiflet 5 wavelet using Soft Thresholding

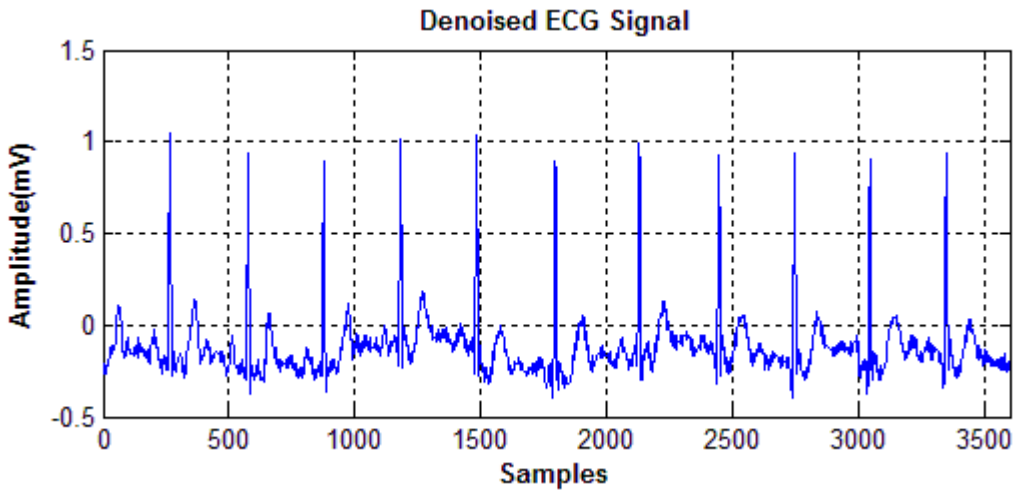

Fig 4.14 Coiflet 4 wavelet using Hard Thresholding

Table 4.4 ECG analysis of Daubechies Mother Wavelet

Daubechies	Soft Thresholding			Hard Thresholding		
	PRD	SNR	MSE	PRD	SNR	MSE
1	0.4047	7.8577	0.0053	0.3301	9.6259	0.0045
2	0.4316	7.298	0.0061	0.33	9.6295	0.0046
3	0.5213	5.6582	0.0086	0.3669	8.7088	0.0055
4	0.4259	7.4143	0.006	0.3263	9.7275	0.0045
5	0.4071	7.8062	0.0056	0.2929	10.6657	0.0037
6	0.5382	5.3814	0.0094	0.4927	6.1489	0.0091
7	0.425	7.4317	0.006	0.5442	5.2854	0.0105
8	0.3369	9.4501	0.0043	0.2839	10.9381	0.0035
9	0.3703	8.6284	0.0051	0.282	10.9964	0.0035
10	0.3387	9.4026	0.0044	0.2905	10.7362	0.0036
11	0.314	10.0625	0.0038	0.2805	11.0405	0.0034
12	0.344	9.2694	0.0044	0.2844	10.9205	0.0035
15	0.2846	10.9138	0.0035	0.2801	11.0545	0.0035
20	0.2889	10.7852	0.0035	0.2816	11.0063	0.0035
25	0.2907	10.7316	0.0036	0.2826	10.9756	0.0035
40	0.2795	11.0712	0.0034	0.2817	11.0043	0.0035

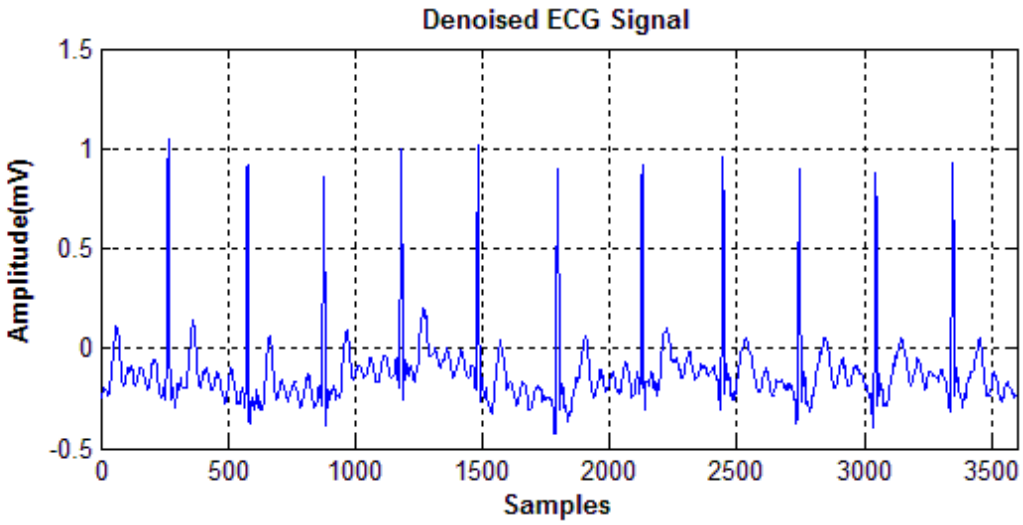

Fig 4.15 Daubechies 40 wavelet using Soft Thresholding

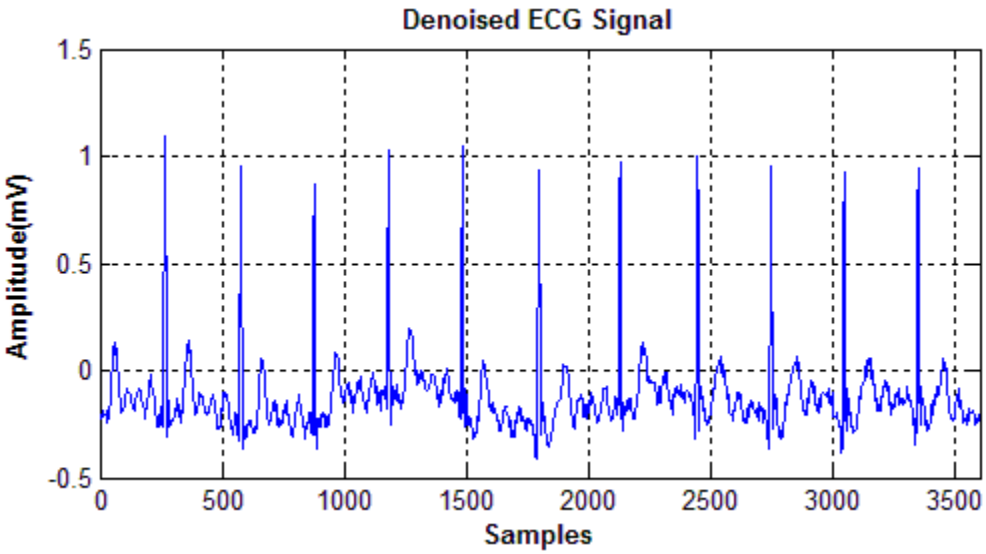

Fig 4.16 Daubechies 15 wavelet using Hard Thresholding

CHAPTER 5

CONCLUSION AND FUTURE SCOPE

Biorthogonal Wavelet Family member, bior3.9 along with soft thresholding technique appears to be the most compatible function among other wavelet function for the denoising of ECG signal using wavelet transform. The functions db40, bior3.9, rbio6.8, sym20 and coif5 gives lesser value of MSE, PRD and larger value of SNR results in their respective family using soft thresholding. The functions db15, bior 2.8, rbio6.8, sym8 and coif4 gives lesser value of MSE, PRD and larger value of SNR results in their respective family using hard thresholding. Wavelets having resembelence with the ECG signals shows better result for removal of noise from ECG signal. By comparing the results of SNR, MSE and PRD of various wavelets we conferred to a result that Hard Thresholding remove noise more effectively as compared to Soft Thresholding.

The results are compared on rigrous sure thresholding technique, for future work results are also compared on heuristic sure, minimax and universal thresholding technique and comparison in term of parameter such as SNR, MSE and PRD.

REFERENCES

[1]. Inderbir Kaur, Rajni and Gaurav Sikri, "Denoising of ECG Signal with Different Wavelets," International Journal of Engineering Trends and Technology (IJETT) – Volume 9 Number 13 - Mar 2014

[2]. Vikramjit Singh, Simranjeet Kaur and Aditi Gupta, "Comparative Study of ECG Signal Denoising and R-peak Registration Methods," International Journal of Engineering Research & Technology (IJERT), ISSN: 2278-0181, Vol. 3 Issue 6, June – 2014

[3]. Uzzal Biswas, Kazi Reyadul Hasan, Biswajit Sana and Md. Maniruzzaman, "Denoising ECG Signal Using Different Wavelet Families and Comparison with Other Techniques," 2nd Int'l Conf. on Electrical Engineering and Information & Communication Technology (ICEEICT) 2015

[4]. Seena V and Jerrin.Yomas, "A REVIEW ON FEATURE EXTRACTION AND DENOISING OF ECG SIGNAL USING WAVELET TRANSFORM," 2014 2nd International Conference on Devices, Circuits and Systems (ICDCS)

[5]. Sarang L. Joshi, Rambabu A.Vatti and Rupali V.Tornekar, "A Survey on ECG Signal Denoising Techniques," 2013 International Conference on Communication Systems and Network Technologies

[6]. J. Pan. and W.J. Tompkins, "A real-time QRS detection algorithm", *IEEE Trans. Biomed. Eng.*, vol. 32,pp 230–236, 1985.

[7]. K. Daqrouq, "ECG base line wander reduction using discrete wavelet transform", Asian Journal of Information Technology, vol. 4, no. 11, pp. 989–995, 2005.

[8]. http://www.physionet.org/physiobank/database/mitdb/ MIT-BIH Database distribution, Massachusetts Institute of Technology, 77 Massachusetts Avenue, Cambridge.

[9]. B. Castro, D. Kogan, and A. B. Geva, "ECG feature extraction using optimal mother wavelet," *21st IEEE Convention of the Electrical and Electronic Engineers* in Israel, pp. 346-350, 2000.

[10]. Y.T. Zhang and R.M. Rangayyan, "Adaptive cancellation of muscle contraction interference in vibroarthrographic signals", IEEE Transactions on Biomedical Engineering, vol. 41, no. 2, pp. 181-191, February 1994

[11]. J. A. Van Alste, T. S. Schilder "Removal of Base-Line Wander and Power-Line Interference from the ECG by an Efficient FIR Filter with a Reduced Number of Taps" *IEEE Transactions On Biomedical Engineering*, vol. bme-32, no. 12, pg no-1052-1060, December 1985.

[12]. Ms. GeetaKadam, Prof.P.C.Bhaskar "Reduction of Power Line Interference in ECG Signal using FIR Filter" *International Journal of Computational Engineering Research* ,ISSN: 2250–3005 Vol. 2 ,Issue No.2, pg no.314-319, ,Mar-Apr 2012.

[13]. S-J.Lee and J.KimM.Lee , "A Real Time ECG Data Compression and Transmission Algorithm for an e-Health Devices". *IEEE Transaction on Biomedical Engineering*vol..58,NO-9 ,September 2011.

[14]. A. K. Barros, A. Mansour and N. Ohnishi, "Removing artifacts from electrocardiographic signals using independent components analysis", Journal of Neuro-computing, vol. 22, no. 1–3, pp. 173–186, 1998.

[15]. Tomas B. Garcia, Neil E. Holtz, "12 Lead ECG: The Art of Interpretation", 2001 edition, Jones & Bartlett publishers, Canada, ISBN-0-7637-1284-1.

[16]. Bracewell RN. The Fourier transform and its applications. McGraw-Hill, 1978.

[17]. Alan V.Oppenheim and Alan S. Willsky. Signal & System. Pearson Education 2nd edition 2004.

[18]. The wavelet Tutorial by RobiPolikar Available: web.iitd.ac.in/~sumeet/WaveletTutorial.pdf.

[19]. B.P.Lathi. Modern Digital and Analog Communication Sytem. **(The Oxford Series in Electrical and Computer Engineering)**

[20]. https://commons.wikimedia.org/wiki/File:ConductionsystemoftheheartwithouttheHeart-en.svg